Nondipole Resonant X-Ray Raman Spectroscopy: Polarized Inelastic Scattering at the K Edge of Cl_2

J. D. Mills,[1] J. A. Sheehy,[1] T. A. Ferrett,[2] S. H. Southworth,[3] R. Mayer,[4]
D. W. Lindle,[5] and P. W. Langhoff[6]
[1]*Propulsion Sciences Division, USAF Phillips Laboratory,Edwards AFB, California 93524-7680*
[2]*Department of Chemistry, Carleton College, Northfield, Minnesota 55057*
[3]*Physics Division, Argonne National Laboratory, Argonne, Illinois 60439*
[4]*Department of Radiation Oncology, Johns Hopkins Hospital, Baltimore, Maryland 21205*
[5]*Department of Chemistry, University of Nevada, Las Vegas, Nevada 89154*
[6]*Department of Chemistry, Indiana University, Bloomington, Indiana 47405*
(Received 9 December 1996)

Experimental and theoretical studies are reported on the inelastic (Raman) scattering of wavelength-selected polarized x rays from the K edge of gas-phase chlorine molecules. The polarized emission spectra exhibit prominent nondipole features consequent of phase variations of the incident and emitted radiation over molecular dimensions, as predicted by the Kramers-Heisenberg scattering formalism. Issues pursuant to the detection of core-hole localization by resonant Raman scattering from homonuclear diatomic molecules are critically examined. [S0031-9007(97)03486-8]

PACS numbers: 33.20.Fb, 33.20.Rm, 33.50.Dq

Measurements of polarized x-ray Raman scattering from the K edges of gas-phase polyatomic molecules were first performed [1–6] at beamline X-24A of the National Synchrotron Light Source employing a double-crystal primary monochromator [7] and a curved-crystal secondary spectrometer with position-sensitive detection [8]. The emission spectra detected along two independent linear polarizations at selected scattering angles provide spectroscopic and dynamical information not easily obtained by other means when appropriately interpreted [1–6,9] employing the Kramers-Heisenberg scattering formalism [10] and its classical limits [11]. The present Letter reports observation of strong *nondipole* features in the polarized x-ray emission spectra of Cl_2 molecules which are quantitatively interpreted with the general scattering formalism and calculations of molecular eigenstates of irreducible symmetry. The scattered intensities depend sensitively upon variations of the phase of the incident and emitted radiation over molecular dimensions, providing structural information directly from the measured emission spectra even in the absence of explicit sample alignment [12,13]. By contrast with the situation in polyatomic molecules, where vibronic coupling can lift the degeneracy of otherwise equivalent core-excited electronic states [14], vibronic core-excited states in homonuclear diatomic molecules remain effectively degenerate. Consequently, resonant x-ray Raman measurements as presently performed are unable to distinguish among irreducible-symmetry or broken-symmetry core-excited states in homonuclear diatomic molecules, contrary to recent assertions in the literature [15,16].

In Fig. 1 is shown the x-ray absorption spectrum of an ambient-temperature low-pressure (≈ 85 Torr) gas sample of Cl_2 recorded near the atomic K edge employing Ge(111) crystals in the double-crystal primary monochromator, providing a spectral resolution of approximately 0.9 eV [7]. The energy scale is calibrated to the position of the strong pre-edge feature at 2821.3 eV as determined by previous measurement [17]. Assignments are made employing the available literature [17,18] and vertical-electronic configuration-interaction calculations reported herein. The pre-edge feature is comprised of two essentially degenerate series of dipole-allowed $X\,^1\Sigma_g^+(\upsilon_\alpha = 0) \rightarrow K_u(\upsilon_\gamma)$ and dipole-forbidden $X\,^1\Sigma_g^+(\upsilon_\alpha = 0) \rightarrow K_g(\upsilon_\gamma)$ excitations nominally attributed to electronic transitions from the doubly occupied K-edge molecular orbitals $(1\sigma_g, 1\sigma_u)$ to the lowest unoccupied orbital $(5\sigma_u)$ [19,20], as summarized in Table I.

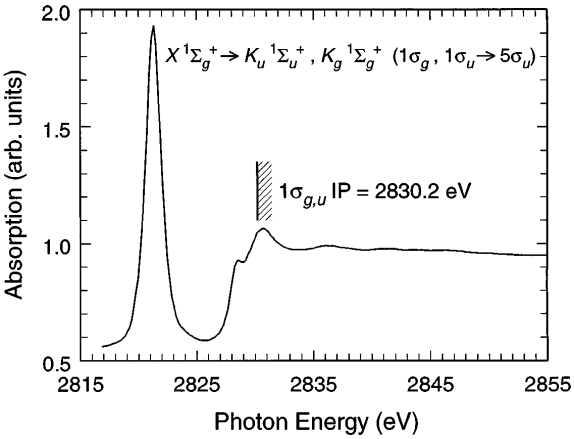

FIG. 1. Measured absorption cross section near the molecular chlorine K edge, calibrated on the basis of the available literature [17,18].

TABLE I. Absorption and Raman transitions in Cl_2.

Transition	Transition energy (eV)[a]	Transition moment (a.u.)[b]
$X \rightarrow K_u\,{}^1\Sigma_u^+(1\sigma_g^{-1}5\sigma_u)$	2819.7 (2821.3)	0.00752
$X \rightarrow K_g\,{}^1\Sigma_g^+(1\sigma_u^{-1}5\sigma_u)$	2819.7 (2821.3)	0.00000
Cl atom $1s \rightarrow 3p$	2815.3 (2815.7)	0.00856
$X \rightarrow X\,{}^1\Sigma_g^+$	0.00 $(\cdots)$	0.00752
$X \rightarrow A^1\Pi_u(2\pi_g^{-1}5\sigma_u)$	4.10 (4.30)	0.00878
$X \rightarrow B^1\Pi_g(2\pi_u^{-1}5\sigma_u)$	6.90 (7.20)	0.00816
$X \rightarrow C_1\,{}^1\Sigma_u^+(2\pi_g^{-1}3\pi_u)$	8.37 $(\cdots)$	$\cdots$
$X \rightarrow C_2\,{}^1\Sigma_u^+(2\pi_g^{-1}4\pi_u)$	9.49 (10.7)	$\cdots$
$X \rightarrow C_3\,{}^1\Sigma_u^+(5\sigma_g^{-1}5\sigma_u)$	12.19 (14.5)	0.00816

[a]Vertical electronic energies relative to the ground state determined by *ab initio* configuration-interaction calculations. Experimental values in parentheses taken from Figs. 1 and 3 for Cl_2; the Cl $1s \rightarrow 3p$ excitation energy is estimated employing the atomic valence-shell ionization potential (13.01 eV) as a term value in the absence of measured data.

[b]Calculated molecular dipole transition moments in absorption and emission for Raman transitions proceeding through the intermediate K_g or K_u states. The diabatic valence transition moment is reported for the C_3 final state.

Theoretical expressions for the two incoherent contributions to the integrated absorption intensity,

$$I_{\mathrm{ab}}\begin{pmatrix} 1\sigma_g \rightarrow 5\sigma_u \\ 1\sigma_u \rightarrow 5\sigma_u \end{pmatrix} \propto 4|\langle 1s|\hat{\mu}_z|5\sigma_u\rangle|^2 \times \left\{\frac{1}{2} \pm \frac{3}{2}\frac{j_1(k_\alpha R_e)}{k_\alpha R_e}\right\}, \quad (1)$$

are obtained from a sum and isotropic average over the individual vibronic absorption strengths which together correspond to the area under the pre-edge resonance feature of Fig. 1. Here, $\hat{\mu}_z$ is the component of the one-electron dipole-moment operator along the body-frame internuclear axis, $1s$ refers to a single atomic component of the $1\sigma_g$ and $1\sigma_u$ symmetry orbitals, and j_1 is a spherical Bessel function dependent upon the product of the radiation wave vector (k_α) and the equilibrium molecular bond distance (R_e). Assumptions employed in Eq. (1) include use of the classical limit of the rotational degrees of freedom, identical Auger-broadened ($\Gamma \approx 0.5$ eV) Lorentzian lineshapes for each vibronic absorption profile, Franck-Condon and closure approximations upon the vibrational degrees of freedom, and an LCAO approximation to the K-edge molecular orbitals [21,22]. The dipole approximation is employed in evaluating the transition moments centered at the two nuclei because the incident wavelength ($\lambda_\alpha = 4.4$ Å) is much larger than the radius ($r_{1s} = 0.032$ Å) of the chlorine core orbital; it is *not* imposed, however, in evaluating transition-moment integrals involving the delocalized symmetry orbitals $1\sigma_g$ and $1\sigma_u$ because the internuclear separation [19] is not negligible relative to the wavelength ($R_e/\lambda_\alpha = 0.45$). The phase variation of the incident radiation over the molecular dimensions must therefore be included [12,13], giving rise to the nondipole structure factors contained in brackets in Eq. (1). Although dipole selection rules are valid in earlier K-edge Raman scattering studies of polyatomic molecules containing a single Cl or S atom [1–6], structure factors can arise in CF_2Cl_2 and $CFCl_3$ in the absence of sufficient vibronic coupling to lift the degeneracy of the equivalent Cl atom core-excited states.

The variation of the structure factors with $k_\alpha R_e$ is displayed in Fig. 2(a). As anticipated, the dipole-allowed $1\sigma_g \rightarrow 5\sigma_u$ component contributes for both small and large values of $k_\alpha R_e$, whereas the $1\sigma_u \rightarrow 5\sigma_u$ component is forbidden in the dipole limit ($k_\alpha \rightarrow 0$). At the value ($k_\alpha R_e = 2.8$) appropriate to the pre-edge resonance feature in Cl_2, however, both transitions contribute significantly, indicating that a multipole expansion of the exponential factor in the electromagnetic-interaction Hamiltonian is inappropriate. Whereas the dipole limit evidently obtains for the corresponding absorption feature in F_2 ($k_\alpha R_e = 0.50$), the hard–x-ray limit ($k_\alpha \rightarrow \infty$) is appropriate to Br_2 ($k_\alpha R_e = 15.6$) and I_2 ($k_\alpha R_e = 45$). Of course, it is not possible to verify these predictions by absorption measurements because *gerade* [$K_g(\upsilon_\gamma)$] and *ungerade* [$K_u(\upsilon_\gamma)$] excited states having common vibrational excitation (υ_γ) are effectively degenerate, and the two nondipole structure factors [Eq. (1)] add incoherently to unity for all values of $k_\alpha R_e$, giving an integrated absorption strength approximately twice that of the resonance transition ($1s \rightarrow np$) in the isolated atom.

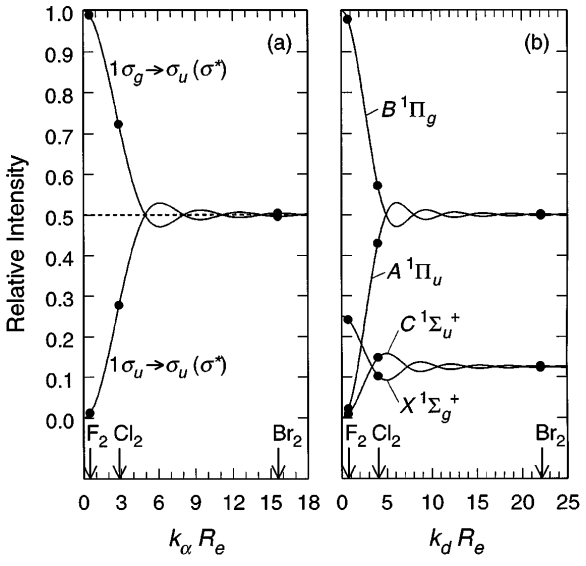

FIG. 2. (a) Variations of the dipole-allowed $X \rightarrow K_u$ and dipole-forbidden $X \rightarrow K_g$ electronic absorption components (—) of the pre-edge resonance for dihalogens [Eq. (1)]. Also shown are components employing localized states (- - -); Eqs. (2) and (3), $\theta = 45°$. (b) Variation of the structure factors of perpendicularly polarized X, A, B, and C Raman emission lines for homonuclear diatomic halogens [Eq. (4)].

The determinantal wave functions comprising the ground and core-excited states in Cl_2 are invariant to the use of unitary broken-symmetry combinations

$$|1\sigma_\theta^{(\pm)}\rangle = \cos\theta|1\sigma_g\rangle \pm \sin\theta|1\sigma_u\rangle, \tag{2}$$

in place of the degenerate symmetric and antisymmetric orbitals $(1\sigma_g, 1\sigma_u)$, and the predicted absorption cross section is invariant to substitution of broken-symmetry combinations

$$|\Phi_\theta^{(\pm)}\rangle = \cos\theta|K_g\rangle \pm \sin\theta|K_u\rangle \tag{3}$$

in place of the degenerate states (K_g, K_u) of irreducible symmetry, although the two individual incoherent contributions will depend upon the rotation angle θ. Figure 2(a) also depicts the two constant and equal structure factors contributing to the absorption cross section obtained employing local-hole states [$\theta = 45°$ in Eqs. (2) and (3)], which factors are seen to sum to unity.

In contrast to the absorption cross section, Raman emission spectra are expected to reveal scattering structure factors consequent of phase variations of the x-ray radiation over molecular dimensions [12,13]. Figure 3 reports such spectra in Cl_2 recorded and analyzed employing procedures described previously [1–6]. The measurements are performed at a scattering angle perpendicular to the directions of incident polarization and propagation along two conventional polarization directions ($\perp, \parallel$) following excitation of the pre-edge resonance ($h\nu_\alpha = 2821.3$ eV). The expected energy resolutions [7] of 0.9 eV for the Ge(111) primary monochromator and 0.4 eV for the Si(111) secondary spectrometer in this range are consistent with the 1.2 eV width observed for the strongest measured peaks, although the continuous nature of final-state vibrations also contributes to spectral broadening [19,20]. The primary and secondary crystals provide essentially absolute linear polarization discrimination in this spectral region [1,4,8], with the measured spectra showing significant polarization dependence. The spectra evidently include strong nondipole two-photon features $X\,^1\Sigma_g^+ \rightarrow K_u/K_g \rightarrow A^1\Pi_u$ and $X \rightarrow K_u/K_g \rightarrow C^1\Sigma_u^+$, as well as dipole-allowed contributions $X \rightarrow K_u \rightarrow X$ and $X \rightarrow K_u \rightarrow B^1\Pi_g$, assignments made on the basis of available literature [19,20] and vertical-electronic calculations (Table I). The nominally forbidden A-state emission lines are seen to have strengths comparable to the dipole-allowed B lines.

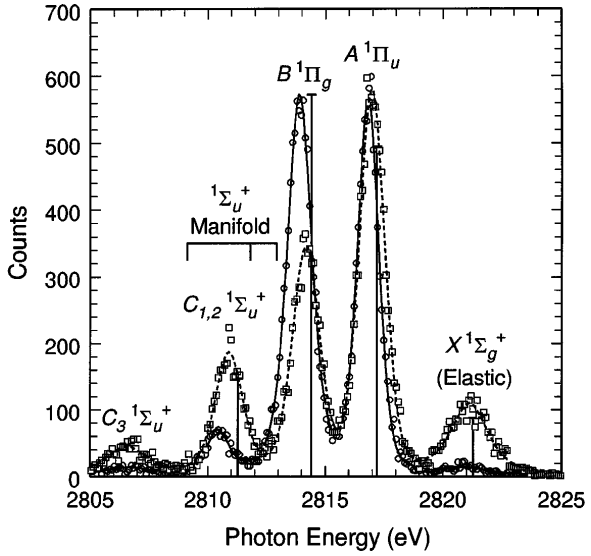

FIG. 3. Raman emission spectra for Cl_2 detected in parallel (□; - - -) and perpendicular (○; —) polarization following excitation of the pre-edge resonance ($h\nu_\alpha \approx 2821$ eV). Predicted integrated intensities for perpendicular polarization are shown as stick heights [Eq. (4) and Table I].

Following procedures similar to those yielding Eq. (1), the Kramers-Heisenberg formula [10,22] provides integrated emission intensities for perpendicular polarization:

$$\begin{aligned} I_{\rm em}^{(\perp)}\begin{pmatrix} X \rightarrow X^1\Sigma_g^+ \\ X \rightarrow C^1\Sigma_u^+ \end{pmatrix} &\propto \left|\left\langle 1s \left| \hat{\mu}_z \right| \begin{matrix} 5\sigma_u \\ 5\sigma_g \end{matrix} \right\rangle\right|^2 \left\{\frac{1}{8} \pm \frac{15}{16}\frac{j_1(k_dR_e)}{k_dR_e} \mp \frac{45}{16}\frac{j_2(k_dR_e)}{(k_dR_e)^2}\right\}, \\ I_{\rm em}^{(\perp)}\begin{pmatrix} X \rightarrow A^1\Pi_u \\ X \rightarrow B^1\Pi_g \end{pmatrix} &\propto \left|\left\langle 1s \left| \hat{\mu}_x \right| \begin{matrix} 2\pi_g \\ 2\pi_u \end{matrix} \right\rangle\right|^2 \left\{\frac{1}{2} \mp \frac{15}{16}\frac{j_1(k_dR_e)}{k_dR_e} \pm \frac{45}{16}\frac{j_2(k_dR_e)}{(k_dR_e)^2}\right\}, \end{aligned} \tag{4}$$

where factors common to each expression have been deleted, $k_d \approx \sqrt{2}\,k_\alpha$ is the magnitude of the difference of incident and scattered wave vectors, and the three C_1- to C_3-state intensities split by valence-Rydberg mixing [20] have been combined into a single diabatic $C\,^1\Sigma_u^+$ state. Predictions for parallel polarization and for other excitation energies are not discussed here.

To the extent that the small differences in the four dipole transition moments can be neglected (Table I), the predicted scattering intensities can be attributed wholly to the diffraction-like structure factors [Eq. (4)] depicted in Fig. 2(b) consequent of the phase variations of incident and scattered radiation over molecular dimensions [12,13]. Evidently, the dipole limit obtains in F_2 ($k_dR_e = 0.71$), whereas Br_2 ($k_dR_e = 22$) and I_2 ($k_dR_e = 63$) are in the hard x-ray limit, in which case the dipole-allowed B and dipole-forbidden A lines have equal intensities that are four times those of the similarly equal X- and C-state features. Chlorine ($k_dR_e = 4.0$) lies in the interval $1 \leq k_dR_e \leq 5$, where structural information (R_e) may be deduced unambiguously from the calculated structure factor.

The predicted integrated intensities shown as stick heights in Fig. 3 are seen to be in good accord with the measured perpendicularly polarized spectrum. Note that

the observed elastic line is depleted by self-absorption and that the predicted diabatic C-state intensity should be compared to the sum of measured intensities in the C_1- to C_3-state interval. The small discrepancies between the measured and predicted spectral positions are presumably due to final-state vibrational excitations not included in the present vertical-electronic calculations.

The Raman emission intensities of Eq. (4) are invariant to unitary choice of the degenerate K-edge orbitals and the degenerate core-excited states K_g and K_u [Eqs. (2) and (3)]. The present results are therefore relevant to the issue of core-hole localization during resonant x-ray Raman scattering [15,16]. It has been asserted that channel interference and core-hole state delocalization occurs in homonuclear diatomic molecules "when the x-ray photon wavelength is comparable or larger than the interatomic distance," whereas in the short wavelength limit "the interference of the localized channels is absent" and the core hole "localizes" to states described by Eqs. (2) and (3) with $\theta = 45^\circ$ [15,16]. The present results [Eq. (4) and Fig. 2(b)], however, apply in both the dipole and hard x-ray limits, and yet are invariant to choice of either localized broken symmetry or delocalized irreducible symmetry descriptions of core-excited states. Accordingly, arguments involving localization or delocalization mechanisms [15,16] are irrelevant to interpretations of resonant x-ray Raman emission measurements on homonuclear diatomic molecules.

This Letter reports observations of strong nondipole emission features in the polarized K-edge Raman spectra obtained from gas-phase Cl_2 molecules. The measured data are in agreement with predictions of the Kramers-Heisenberg scattering formalism, which provides nondipole x-ray structure factors consequent of phase variations of the incident and emitted radiation over molecular dimensions. The reported data do not require or support special core-hole localization or delocalization mechanisms [15,16], circumstances which are not detected by x-ray Raman emission measurements as presently performed on gas-phase homonuclear diatomic molecules.

The U.S. Air Force Office of Scientific Research provided a Palace-Knight Fellowship to J. D. M. and a University Resident Research Professorship to P. W. L. This work was also funded by the U.S. Department of Energy Office of Basic Sciences under Contract No. W-31-109-Eng-38. We thank R. D. Deslattes for his continuing support and encouragement, and we acknowledge the collaboration of our late colleague Paul Cowan.

[1] D. W. Lindle, P. L. Cowan, R. E. LaVilla, T. Jach, R. D. Deslattes, B. Karlin, J. A. Sheehy, T. J. Gil, and P. W. Langhoff, Phys. Rev. Lett. **60**, 1010 (1988).
[2] D. W. Lindle, P. L. Cowan, T. Jach, R. E. LaVilla, R. D. Deslattes, and R. C. C. Perera, Phys. Rev. A **43**, 2353 (1991).
[3] R. C. C. Perera, P. L. Cowan, D. W. Lindle, R. E. LaVilla, T. Jach, and R. D. Deslattes, Phys. Rev. A **43**, 3609 (1991).
[4] S. H. Southworth, D. W. Lindle, R. Mayer, and P. L. Cowan, Phys. Rev. Lett. **67**, 1098 (1991).
[5] S. H. Southworth, D. W. Lindle, R. Mayer, and P. L. Cowan, Nucl. Instrum. Methods Phys. Res., Sect. B **56/57**, 304 (1991).
[6] R. Mayer, D. W. Lindle, S. H. Southworth, and P. L. Cowan, Phys. Rev. A **43**, 235 (1991).
[7] P. L. Cowan, S. Brennan, R. D. Deslattes, A. Henins, T. Jach, and E. G. Kessler, Nucl. Instrum. Methods Phys. Res., Sect. A **246**, 154 (1986).
[8] S. Brennan, P. L. Cowan, R. D. Deslattes, A. Henins, D. W. Lindle, and B. A. Karlin, Rev. Sci. Instrum. **60**, 2243 (1989).
[9] P. L. Cowan, in *Resonant Anomalous X-Ray Scattering: Theory and Applications*, edited by G. Materlik, C. J. Sparks, and K. Fischer (North-Holland, Amsterdam, 1994), pp. 449–472.
[10] W. Heitler, *The Quantum Theory of Radiation* (Clarendon, Oxford, 1954).
[11] R. N. Zare, *Angular Momentum* (Wiley, New York, 1988).
[12] Y. Ma, Chem. Phys. Lett. **230**, 451 (1994). Equations (2) to (4) in this reference apply to the elastic $X \rightarrow X$ Raman transition and not to the $X \rightarrow C$ transition as asserted.
[13] Y. Ma, Phys. Rev. B **49**, 5799 (1994).
[14] L. S. Cederbaum, J. Chem. Phys. **103**, 562 (1995).
[15] F. Gel'mukhanov and H. Ågren, Phys. Rev. A **49**, 4378 (1994).
[16] P. Glans, K. Gunnelin, P. Skytt, J. H. Guo, N. Wassdahl, J. Nordgren, H. Agren, F. Gel'mukhanov, T. Warick, and E. Rotenberg, Phys. Rev. Lett. **76**, 2448 (1996).
[17] S. Bodeur, J. L. Marèchal, C. Reynard, D. Bazin, and I. Nenner, Z. Phys. D **17**, 291 (1990).
[18] D. L. Foulis, R. F. Pettifer, and P. Sherwood, Europhys. Lett. **29**, 647 (1995).
[19] K. P. Huber and G. Herzberg, *Constants of Diatomic Molecules* (Van Nostrand, New York, 1979).
[20] S. D. Peyerimhoff and R. J. Buenker, Chem. Phys. **57**, 279 (1981).
[21] J. D. Mills and P. W. Langhoff, in *Raman Emission by X-Ray Scattering*, edited by D. L. Ederer and J. H. McGuire (World Scientific, River Edge, NJ, 1996), pp. 169–192.
[22] J. D. Mills, Ph.D. Dissertation, Indiana University, Bloomington, IN (1997).